IEEE Photonics Journal
An IEEE Photonics Society Publication

Electro-Refraction Modulation Predictions for Silicon Graphene Waveguides in the 1540–1560 nm Region

Volume 8, Number 5, October 2016

Daniel Pérez
David Domenech
Pascual Muñoz, ***Senior Member, IEEE***
José Capmany, ***Fellow, IEEE***

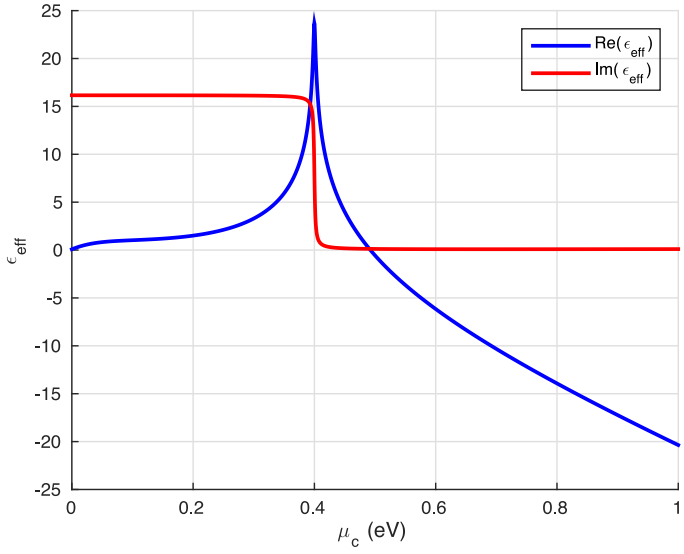

DOI: 10.1109/JPHOT.2016.2598781
1943-0655 © 2016 IEEE

Electro-Refraction Modulation Predictions for Silicon Graphene Waveguides in the 1540–1560 nm Region

Daniel Pérez,[1] **David Domenech,**[2]
Pascual Muñoz,[1] ***Senior Member, IEEE*,**
and José Capmany,[1] ***Fellow, IEEE***

[1]Institute of Telecommunications and Multimedia, Universitat Politecnica de Valencia, Valencia 46021, Spain.
[2]VLC Photonics S.L., Camino de Vera s/n, 46022 Valencia, Spain.

DOI:10.1109/JPHOT.2016.2598781

Manuscript received July 20, 2016; revised August 4, 2016; accepted August 5, 2016. Date of publication August 10, 2016; date of current version September 2, 2016. This work was supported in part by the Research Excellency Award Program GVA PROMETEO II/2013/012; in part by Spanish MINECO projects TEC2013-42332-P PIF4ESP, TEC2015-69787-REDT PIC4TB, and TEC2014-60378-C2-1-R MEMES; and in part by projects FEDER UPVOV 10-3E-492 and FEDER UPVOV 08-3E-008. The work of D. Pérez was supported by the FPI-UPV Grant Program from the Universitat Politècnica de València.
Corresponding author: J. Capmany (e-mail: jcapmany@iteam.upv.es).

Abstract: We derive analytical approximations for the variation of the effective indices of the fundamental transverse electric (TE) and transverse magnetic (TM) modes with the chemical potential of graphene in three common types of silicon graphene waveguides. In all cases, a third-order polynomial provides an excellent degree of approximation ($< 10^{-4}$) over the 1540–1560 nm wavelength band. The approximations can be useful in the design of complex-integrated photonic circuits where graphene is employed to tune the refractive of the dielectric waveguides.

Index Terms: Graphene, integrated optics, Microwave photonics

1. Introduction

Graphene is a 2-D single layer of carbon atoms arranged in an hexagonal lattice that has raised considerable interest in recent years due to its remarkable optical and electronic properties [1]–[3]. It features, for instance, a linear dispersion relationship in the so-called Dirac points where electrons behave as fermions with zero mass, propagating at a speed of around 10^6 m s^{-1} and mobility values of up to 10^6 $cm^2V^{-1}s^{-1}$. Graphene also shows unusual optical properties [4]. For instance, due to its linear dispersion, it can absorb light over a broad frequency range enabling broadband applications. In addition, the density of states of carriers near the Dirac point is low, and as a consequence, its Fermi energy can be tuned significantly with relatively low electrical energy (applied voltage) [1]–[4]. This Fermi level tuning changes, in turn, the refractive index of graphene, and thus, the combination of graphene with integrated dielectric waveguides opens unprecedented possibilities for the design of tunable components in optoelectronics [5] and several groups have recently reported devices with applications in the microwave, terahertz and photonic regions of the electromagnetic spectrum [3]–[6]. A particularly active area of research aims at designing tunable integrated photonic components, and different groups have reported

both theoretical and experimental contributions addressing different functionalities that include electro-absorption modulation in straight waveguides [6]–[8], resonant modulators [9], channel switching [10], and electro-refractive modulation [11]–[14]. Electro-refractive modulation is particularly interesting since phase modulation enables additional functionalities, such as phase shifting and true time delaying [15], which are highly desirable in the design of tunable optical filters [16] and in microwave photonics [17].

The design of tunable electro-refractive phase shifters in a silicon graphene waveguide of length L at a wavelength λ requires the knowledge of the dependence of the phase shift $\phi = (2\pi n_{\text{eff}}/\lambda)L$ imposed by the waveguide on a control parameter, in this case, the chemical potential μ_c of graphene, as the effective index of the guided mode n_{eff} is a function of this parameter. In general, this relationship can only be obtained for a given wavelength by numerical means of a modal solver and repeating this process within the wavelength region of interest. The motivation of our work resides in the fact that for the design of graphene based devices featuring some degree of complexity (modulators, finite and infinite impulse response optical filters, phase-shifters and true time delay lines, etc.), it is useful to dispose of approximate analytical expression for the variation of n_{eff} with μ_c as these will facilitate the higher-level design process (for instance, the filter synthesis). This approach has also been followed as well, for instance, to render expressions to approximate the impact that free carrier injection has on electroabsorption and electro-refraction in silicon waveguides [18]. The difference here is that the approximation not only depends on the properties of graphene, but it is also linked to the specific waveguide design. We have therefore chosen three respresentative waveguide designs that have been reported in the literature [6], [12] for the implementation of graphene based modulators. This is in principle a limitation, but in the paper, we also outline the process to extend these analytical approximations to other waveguide designs.

In this paper we provide analytical approximate relationships in the 1540–1560 nm wavelength range between the value of the chemical potential and the effective index of transverse electric (TE) and transverse magnetic (TM) (where applicable) fundamental modes for three different types of Silicon waveguides that have been proposed in the literature to implement silicon graphene electro-refractive modulators. After briefly reviewing basic aspects of the conductivity and dielectric constant of graphene we describe in Section III, the three types of silicon waveguides considered in the paper, including their physical dimensions and materials. In Section IV, we carry out the numerical calculations for each type of waveguide and provide the polynomial approximations. In all the cases, the modal effective index can be approximated by means of a seventh-order polynomial with an excellent precision (i.e better than 10^{-4}). For completeness, we also provide the polynomial approximation for the absorption coefficient (expressed in dB/mm) where the precision is in the range of 10^{-2}. Finally, we discuss the results and provide a summary in Section V.

2. Graphene Refractive Index Versus Chemical Potential

Graphene is a material with noteworthy optical properties due to its conical band structure that allows both intra-band and inter-band transitions [1]–[3], both contributing to its conductivity [19]

$$\sigma(\omega) = \sigma_{\text{intra}}(\omega) + \sigma_{\text{inter}}(\omega) \tag{1}$$

Intra-band transitions are the dominant source for the overall conductivity in the microwave and terahertz regions of the spectrum and their contribution can be expressed in terms of the Kubo's formula [19]

$$\sigma_{\text{intra}}(\omega) = \frac{ie^2 k_B T}{\pi\hbar^2 (\omega + i2\Gamma)} \left[\frac{\mu_c}{k_B T} + 2\ln\left(e^{-(\mu_c/k_B T)} + 1\right) \right] \tag{2}$$

where e represents the charge of the electron, $\hbar$ the angular Planck constant, k_B the Boltzman constant, T the temperature, μ_c the Fermi level or chemical potential, and

$$\Gamma = \frac{e\mathbf{v_F^2}}{\mu\mu_c} \tag{3}$$

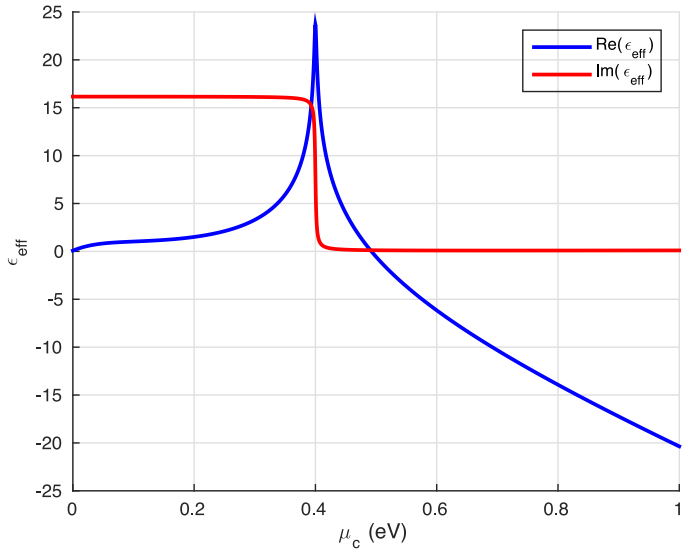

Fig. 1. Real and imaginary parts of graphene refractive index of the dielectric constant of a layer of graphene for $\lambda = 1550$ nm, $T = 300^{\circ}K$, and $1/2\Gamma = 5 \times 10^{-13}$ sec as a function of the chemical potential.

is the electron collision rate, which is a function of the electron mobility μ and the Fermi velocity in graphene $\mathbf{v_F} \approx 10^6$ ms^{-1}. In the visible optical region of the spectrum, however, inter-band transitions dominate the conductivity that is given if $k_B T << |\mu_c|, \hbar\omega$ by [13]

$$\sigma_{\text{inter}}(\omega) = \frac{ie^2\omega}{\pi} \int_0^{\infty} \frac{f(x-\mu_c) - f(-x-\mu_c)}{4x^2 - (\hbar\omega + i\Gamma)^2} dx \tag{4}$$

where $f(x)$ is the Fermi-Dirac distribution

$$f(x) = \frac{1}{\exp\left[\frac{(x-\mu_c)}{k_B T}\right] + 1} \tag{5}$$

From (1)–(5), one can get the dielectric constant of a layer of graphene:

$$\varepsilon_{\text{eff}}(\omega) = 1 + \frac{i\sigma(\omega)}{\omega\varepsilon_o\Delta} \tag{6}$$

where $\Delta = 0.35$ nm is the thickness of the layer. Fig. 1 represents as an example, the real and imaginary parts of the dielectric constant of a layer of graphene for $\lambda = 1550$ nm, $T = 300^{\circ}$K, and $1/2\Gamma = 5 \times 10^{-13}$ sec as a function of the chemical potential.

In this particular example, a transition can be observed at $|\mu_c| = 0.4$ eV, where the dielectric constant changes from dominantly imaginary $|\mu_c| < 0.4$ eV, to purely real $|\mu_c| > 0.4$ eV. Note that 0.4 eV corresponds to the energy associated with $\lambda/2(\lambda = 1550$ nm) and thus this chemical potential sets the onset of interband absorption in graphene. Thus, for $|\mu_c| > 0.4$ eV graphene becomes electro-refractive. On the other side, a small change in the chemical potential in both directions around $|\mu_c| = 0.4$ eV yields a substantial change in the imaginary value of the dielectric constant (i.e the losses) and graphene is electro-absorptive in that region. Exploiting the electro-refractive behaviour with a constant low absorption value of graphene lies at the heart of designing modulators, tunable phase shifters, and delay lines, which are fundamental building blocks of more elaborated subsystems such as, for instance tunable photonic filters. In practice, however, it has been noticed [12], [13] that the region 0.4 eV $< |\mu_c| <$ 0.5 eV features a considerable non-constant absorption, therefore the region for true electro-refractive behavior is $|\mu_c| > 0.5$ eV, which is the one we consider in this paper. The refractive index variation in region 0.4 eV $< |\mu_c| <$ 0.5 eV can

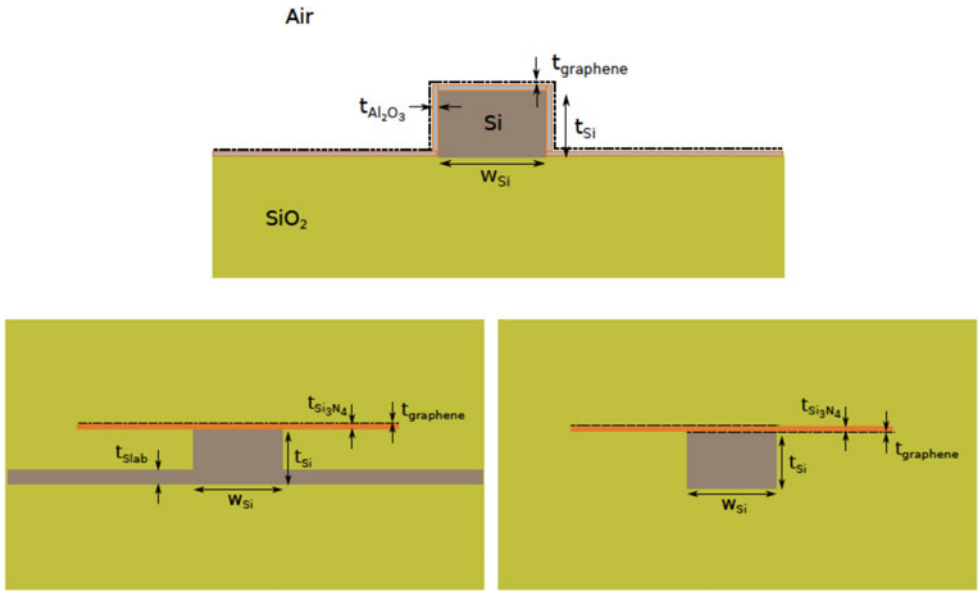

Fig. 2. Typical silicon graphene waveguide designs reported in the literature and considered in this study. (top) Type-I, deep silicon waveguide with a single layer of graphene on top of it separated by an Al_2O_3 dielectric layer. (Bottom left): Type-II, buried silicon waveguide with a single layer of graphene on top of it separated by an Si_3N_4 dielectric layer. (Bottom right): Type-III, buried silicon waveguide with a double layer of graphene on top of it separated by an Si_3N_4 dielectric layer.

still be approximated by a polynomial but to obtain a similar approximation error a seventh-order polynomial is required.

3. Silicon Graphene Waveguides

Modulators and tunable phase shifters and delay lines can be implemented by incorporating Graphene into silicon waveguide designs. In this paper, we consider three typical representative designs that have been proposed in the literature, which are shown in Fig. 2.

The first design (Type-I), shown in the upper part of Fig. 2 was reported in [6] for an electroabsorption modulator and consists in placing a monolayer graphene sheet on top of a silicon bus waveguide, separated from it by a thin Al_2O_3 dielectric layer. The typical values for the dimensions in this configuration are: $t_{Si} = 250$ nm, $t_{Al_2O_3} = 10$ nm, $t_{graphene} = 0.35$ nm, and $W_{Si} = 500$ nm. The structure was operated by means of two gold electrodes placed at both sides of the silicon waveguides. One of them is extended towards the waveguide by extending a platinum film on top of the graphene layer (see more details in [6]). The designs shown respectively in the left and right lower part of Fig. 2 correspond to a single (Type-II) and double (Type-III) graphene layer silicon waveguides optimized for electro-refractive modulation operation [12], where the dielectric separating the graphene and the silicon waveguide (left) and the two graphene layers (right) is Si_3N_4. The typical values for the dimensions are: $t_{Si} = 160$ nm, $t_{Si_3N_4} = 10$ nm, $t_{slab} = 60$ nm, $t_{graphene} = 0.35$ nm, and $W_{Si} = 480$ nm for the single graphene layer waveguide and $t_{Si} = 220$ nm, $t_{Si_3N_4} = 10$ nm, $t_{graphene} = 0.35$ nm, and $W_{Si} = 480$ nm for the double graphene layer waveguide. These designs are representative of the two main approaches reported so far for the implementation of graphene based silicon modulators. Type-I and variants based on using Al_2O_3 as insulator are reported in [1], [7], and [13], where historically the first choice. However, Type-II and III rely on using Si_3N_4 and have been proposed more recently [12] as this material provides a higher value of dielectric constant and therefore requires an electric field value to reach the $|\mu_c| > 0.5$ eV region which is less close to its breakdown value.

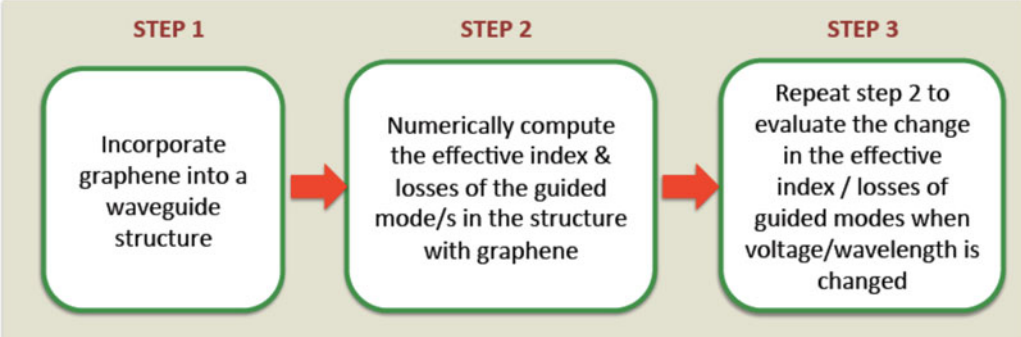

Fig. 3. Three steps involved in the modal solution of graphene silicon waveguides.

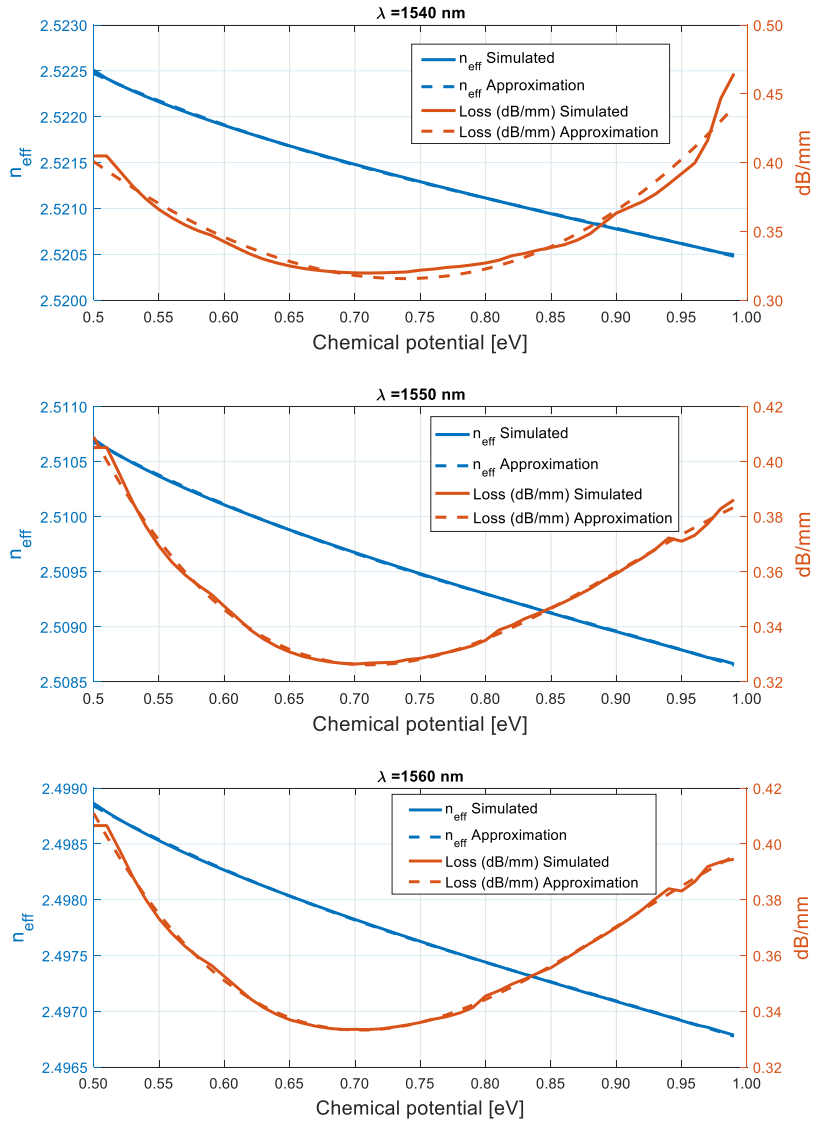

Fig. 4. Numerical computation results (solid blue)/(solid red) and polynomial approximation (broken trace blue)/(broken trace red) for the effective index/ absorption coefficient of the fundamental TE mode in a Type-I waveguide versus the value of the chemical potential. Results are shown for the lowest, middle, and highest wavelength in the range of interest.

TABLE I
Coefficients for the Fitting Polynomial [see (7)] for the TE Mode of Type-I Silicon Graphene Waveguide

	Effective Index (n_{eff})					Propagation Losses (dB/mm)				
$\lambda(\mu m)$	a	b	c	d	δE-06	a*	b*	c*	d*	δE-03
1.540	−0.007	0.019	−0.020	2.529	8.44	0.895	−0.254	−1.084	0.895	7.03
1.541	−0.007	0.019	−0.020	2.527	8.26	−0.077	1.750	−2.437	1.193	5.18
1.542	−0.007	0.019	−0.020	2.526	8.10	−0.766	3.177	−3.401	1.407	3.89
1.543	−0.007	0.019	−0.020	2.525	7.97	−1.263	4.204	−4.094	1.560	3.05
1.544	−0.007	0.019	−0.020	2.524	7.87	−1.641	4.984	−4.620	1.676	2.53
1.545	−0.007	0.019	−0.020	2.523	7.81	−1.948	5.621	−5.050	1.771	2.24
1.546	−0.007	0.019	−0.020	2.521	7.73	−2.184	6.110	−5.379	1.843	2.13
1.547	−0.007	0.019	−0.020	2.520	7.65	−2.305	6.353	−5.535	1.876	2.03
1.548	−0.007	0.019	−0.020	2.519	7.56	−2.322	6.367	−5.530	1.873	1.85
1.549	−0.007	0.019	−0.020	2.518	7.47	−2.307	6.313	−5.478	1.858	1.67
1.550	−0.007	0.019	−0.020	2.517	7.38	−2.309	6.301	−5.458	1.851	1.54
1.551	−0.007	0.019	−0.020	2.516	7.30	−2.340	6.359	−5.490	1.857	1.44
1.552	−0.007	0.019	−0.020	2.514	7.22	−2.392	6.464	−5.556	1.871	1.38
1.553	−0.007	0.018	−0.020	2.513	7.15	−2.446	6.573	−5.627	1.886	1.36
1.554	−0.007	0.018	−0.020	2.512	7.11	−2.494	6.674	−5.693	1.900	1.38
1.555	−0.007	0.018	−0.019	2.511	7.08	−2.547	6.788	−5.771	1.917	1.48
1.556	−0.007	0.018	−0.019	2.510	7.05	−2.601	6.908	−5.855	1.936	1.66
1.557	−0.007	0.018	−0.019	2.508	7.00	−2.615	6.943	−5.879	1.942	1.78
1.558	−0.007	0.018	−0.019	2.507	6.94	−2.541	6.783	−5.766	1.916	1.70
1.559	−0.007	0.018	−0.019	2.506	6.89	−2.404	6.487	−5.557	1.868	1.49
1.560	−0.007	0.018	−0.019	2.505	6.83	−2.262	6.186	−5.346	1.820	1.34

4. Numerical Calculations and Polynomial Approximation

4.1. General Remarks

For all the three waveguide designs, the presence of the graphene layer modifies the propagation characteristics (field profile, losses, and effective index) of the guided modes in the waveguide, and these can be, as mentioned above, controlled and reconfigured changing the chemical potential by means of applying a suitable voltage. In addition, all these properties are wavelength dependent, and therefore, a complete description of how these parameters change in terms of chemical potential and wavelength is required. With the exception of very simple (and unpractical) slab waveguide configurations, this description requires the completion of the three steps described in Fig. 3, which involve the use of numerical or mode solving techniques.

In our case, the TE and (if applicable) the TM modes of the waveguides have been numerically calculated by means of a Finite Differences (FD) based commercial Field Designer^{TM} mode solver from PhoeniX Software B.V. The refractive indices (@1550 nm) for the different materials are 1.746 for Al_2O_3, 3.477 for Si and 1.979 for Si_3N_4. The dispersive nature of the materials has been taken into account in the numerical calculations in the wavelength range under study (1540–1560 nm) by means of the corresponding Sellmeier equations and coefficients. Graphene has been modeled as an isotropic material.

TABLE II
Coefficients for the Fitting Polynomial [see (7)] for the TM Mode of Type-I Silicon Graphene Waveguide

	Effective Index (n_{eff})					Propagation Losses (dB/mm)				
λ (μm)	a	b	c	d	δE-05	a*	b*	c*	d*	δE-02
1.540	−0.042	0.104	−0.095	1.906	11.00	−32.389	86.865	−74.690	22.212	11.20
1.541	−0.041	0.101	−0.093	1.903	10.40	−35.459	92.370	−77.777	22.748	10.30
1.542	−0.040	0.099	−0.091	1.901	9.79	−37.170	95.128	−79.049	22.893	9.51
1.543	−0.038	0.096	−0.089	1.898	9.27	−37.699	95.511	−78.764	22.705	8.89
1.544	−0.037	0.093	−0.087	1.896	8.80	−37.581	94.617	−77.658	22.345	8.37
1.545	−0.036	0.091	−0.085	1.894	8.38	−37.151	93.135	−76.193	21.914	7.91
1.546	−0.035	0.089	−0.083	1.891	7.99	−36.576	91.405	−74.594	21.461	7.50
1.547	−0.035	0.087	−0.082	1.889	7.64	−35.943	89.599	−72.975	21.011	7.13
1.548	−0.034	0.085	−0.080	1.887	7.31	−35.305	87.823	−71.403	20.578	6.79
1.549	−0.033	0.084	−0.079	1.884	7.00	−34.697	86.144	−69.923	20.171	6.47
1.550	−0.033	0.082	−0.078	1.882	6.72	−34.136	84.596	−68.556	19.794	6.17
1.551	−0.032	0.081	−0.077	1.880	6.46	−33.619	83.174	−67.298	19.447	5.88
1.552	−0.031	0.080	−0.076	1.878	6.22	−33.111	81.795	−66.091	19.116	5.60
1.553	−0.031	0.078	−0.075	1.876	6.00	−32.494	80.202	−64.750	18.758	5.35
1.554	−0.030	0.077	−0.074	1.874	5.80	−31.662	78.162	−63.113	18.337	5.12
1.555	−0.030	0.076	−0.073	1.871	5.62	−30.695	75.845	−61.297	17.878	4.91
1.556	−0.029	0.074	−0.072	1.869	5.44	−29.754	73.598	−59.540	17.435	4.71
1.557	−0.029	0.073	−0.071	1.867	5.28	−28.925	71.603	−57.968	17.036	4.52
1.558	−0.028	0.073	−0.071	1.865	5.12	−28.227	69.902	−56.608	16.685	4.34
1.559	−0.028	0.072	−0.070	1.863	4.96	−27.661	68.493	−55.459	16.383	4.17
1.560	−0.028	0.071	−0.069	1.861	4.82	−27.230	67.387	−54.529	16.132	3.99

We have found, after extensive simulations for the region of electrorefractive behavior is $|\mu_c| > 0.5$ eV, that the refractive index modulation and the absorption coefficient can be both approximated with a remarkable precision in the three silicon graphene waveguide designs by a third-order polynomial as a function of the chemical potential:

$$n_{\text{eff}}^{TE/TM}(\mu_c) \approx a\mu_c^3 + b\mu_c^2 + c\mu_c + d$$
$$\alpha^{TE/TM}(\mu_c) \approx a^*\mu_c^3 + b^*\mu_c^2 + c^*\mu_c + d^* \quad (7)$$

where the coefficients *a,b,c,d* and $a\times, b\times, c\times, d\times$ depend on the waveguide configuration, the operating wavelength, and the mode polarization. In the following subsections, we present the results for each type of waveguide.

4.2. Results for Type-I Waveguides

The numerical procedure described above was carried within the 1540–1560 nm wavelength region (using a 1 nm step) and results obtained for the variation of the effective indexes vs the chemical potential for the TE and TM fundamental modes, both of which are supported by Type-I waveguide. Fig. 4 plots as an example the results corresponding to the numerical solution and the fitting polynomial interpolation of the variation of the effective index for the TE fundamental mode as a

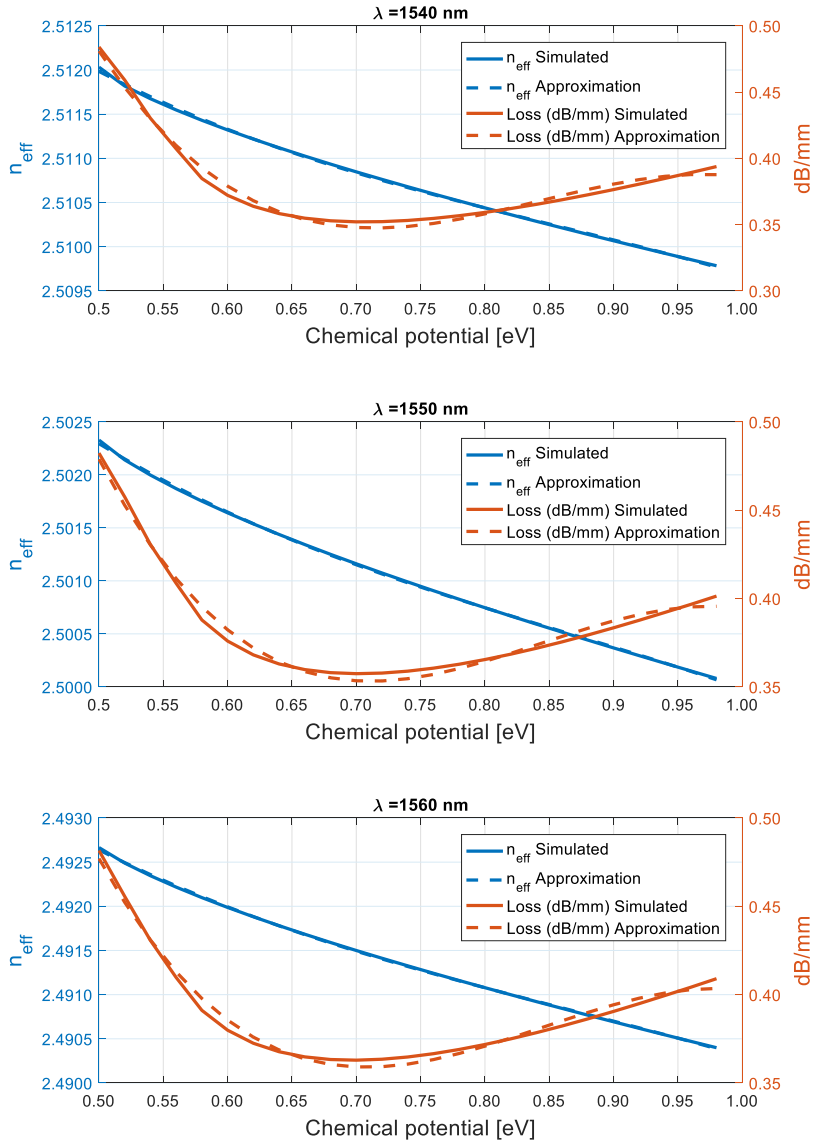

Fig. 5. Numerical computation results (solid blue)/(solid red) and polynomial approximation (broken trace blue)/(broken trace red) for the effective index/ absorption coefficient of the fundamental TE mode in a Type-II waveguide versus the value of the chemical potential. Results are shown for the lowest, middle, and highest wavelength in the range of interest.

function of the chemical potential and different operation wavelengths (1540, 1550, and 1560 nm). Due to space constraints we only show the results for these three wavelengths, but Table I provides the value of the coefficients for the fitting polynomial for the 1 nm spaced wavelengths and provides, for each one, the mean approximation error δ in its last column. In a similar way, results have been obtained for the TM mode (not shown here), which result in the coefficients for the fitting polynomial shown in Table II. In both cases, the approximation is excellent with a mean error value $\delta < 10^{-4}$ and with a better approximation of the TE than for the TM mode.

4.3. Results for Type-II Waveguides

The numerical procedure described above was carried within the 1540-1560 nm wavelength region (using a 1 nm step) and results obtained for the variation of the effective indexes vs the chemical

TABLE III
Coefficients for the Fitting Polynomial [see (7)] for the TE Mode of Type-II Silicon Graphene Waveguide

	Effective Index (n_{eff})					Propagation Losses (dB/mm)				
λ (μm)	a	b	c	d	δE-05	a*	b*	c*	d*	δE-03
1.540	−0.011	0.027	−0.027	2.520	1.69	−4.880	12.322	−10.134	3.077	4.55
1.541	−0.010	0.027	−0.026	2.519	1.63	−4.853	12.256	−10.079	3.063	4.51
1.542	−0.010	0.026	−0.026	2.518	1.57	−4.827	12.191	−10.026	3.049	4.48
1.543	−0.010	0.026	−0.026	2.517	1.52	−4.801	12.129	−9.974	3.035	4.44
1.544	−0.010	0.026	−0.026	2.516	1.47	−4.776	12.068	−9.924	3.022	4.41
1.545	−0.010	0.025	−0.025	2.515	1.43	−4.752	12.009	−9.875	3.009	4.38
1.546	−0.010	0.025	−0.025	2.514	1.39	−4.729	11.952	−9.829	2.997	4.35
1.547	−0.010	0.025	−0.025	2.513	1.35	−4.707	11.898	−9.784	2.985	4.33
1.548	−0.010	0.025	−0.025	2.512	1.31	−4.686	11.847	−9.742	2.974	4.30
1.549	−0.009	0.025	−0.025	2.511	1.28	−4.666	11.798	−9.702	2.964	4.28
1.550	−0.009	0.024	−0.025	2.510	1.25	−4.647	11.752	−9.663	2.954	4.26
1.551	−0.009	0.024	−0.025	2.509	1.23	−4.629	11.705	−9.625	2.944	4.24
1.552	−0.009	0.024	−0.024	2.508	1.20	−4.609	11.657	−9.585	2.933	4.22
1.553	−0.009	0.024	−0.024	2.507	1.18	−4.588	11.605	−9.542	2.922	4.19
1.554	−0.009	0.024	−0.024	2.506	1.16	−4.565	11.550	−9.496	2.910	4.16
1.555	−0.009	0.024	−0.024	2.505	1.14	−4.543	11.493	−9.449	2.897	4.13
1.556	−0.009	0.023	−0.024	2.504	1.12	−4.520	11.438	−9.403	2.885	4.10
1.557	−0.009	0.023	-0.024	2.503	1.10	−4.499	11.384	−9.358	2.873	4.08
1.558	−0.009	0.023	−0.024	2.502	1.08	−4.478	11.333	−9.316	2.862	4.05
1.559	−0.009	0.023	−0.024	2.501	1.07	−4.458	11.284	−9.275	2.851	4.03
1.560	−0.009	0.023	−0.024	2.500	1.05	−4.440	11.238	−9.236	2.841	4.01

potential for the TE fundamental mode, which is the only one supported by Type-II waveguide. In this case, we have used a homogeneous doping level for signal, that is, we did not take into account the effect of inhomogeneous charge distribution in the silicon region close to the Si-Si_3N_4 interface. This effect will tend to inhomogeneously decrease the refractive index in that region and should be taken into account for a more precise description. Fig. 5 plots as an example the results corresponding to the numerical solution and the fitting polynomial interpolation of the variation of the effective index for the TE fundamental mode as a function of the chemical potential and different operation wavelengths (1540, 1550, and 1560 nm).

Again, due to space constraints, we only show the results for these three wavelengths, but Table III provides the value of the coefficients for the fitting polynomial for the 1 nm spaced wavelengths and also provides, for each one, the mean approximation error δ in its last column. Again, an excellent approximation, this time with a mean error value $\delta < 2 \times 10^{-5}$, is obtained.

4.4. Results for Type-III Waveguides

Again, the numerical procedure described above was carried within the 1540–1560 nm wavelength region (using a 1 nm step) and results obtained for the variation of the effective indexes vs the chemical potential for the TE and TM fundamental modes, which are supported by Type-III wave-

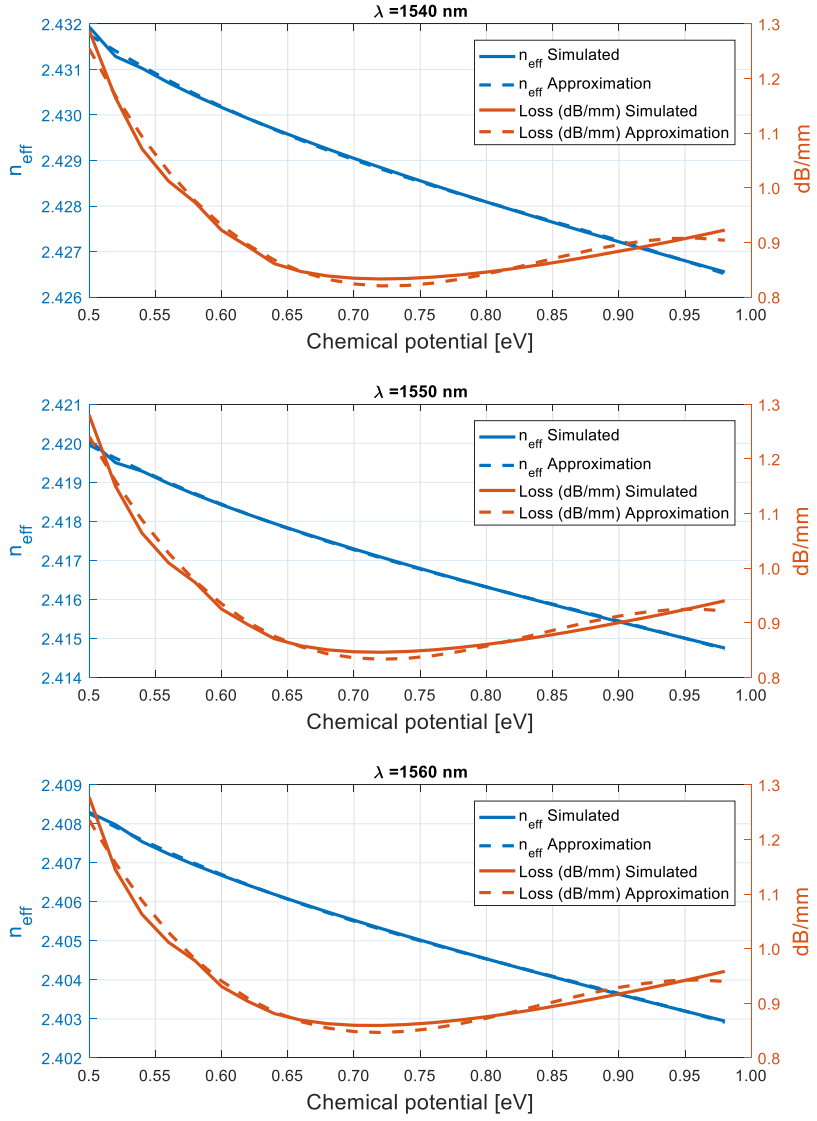

Fig. 6. Numerical computation results (solid blue)/(solid red) and polynomial approximation (broken trace blue)/(broken trace red) for the effective index/ absorption coefficient of the fundamental TE mode in a Type-III waveguide versus the value of the chemical potential. Results are shown for the lowest, middle, and highest wavelength in the range of interest.

guide. Fig. 6 plots as an example the results corresponding to the numerical solution and the fitting polynomial interpolation of the variation of the effective index for the TE fundamental mode as a function of the chemical potential and different operation wavelengths (1540, 1550, and 1560 nm). Due to space constraints, we only show the results for these three wavelengths, but Table IV provides the value of the coefficients for the fitting polynomial for the 1 nm spaced wavelengths and also provides, for each one, the mean approximation error δ in its last column. In a similar way, results have been obtained for the TM mode (not shown here), which result in the coefficients for the fitting polynomial shown in Table V. In both cases, the approximation is excellent with a mean error value $\delta < 3 \times 10^{-4}$ and with a better approximation of the TE than for the TM mode.

TABLE IV
Coefficients for the Fitting Polynomial [see (7)] for the TE Mode of Type-III Silicon Graphene Waveguide

	Effective Index (n_{eff})					Propagation Losses (dB/mm)				
λ (μm)	a	b	c	d	δE-05	a*	b*	c*	d*	δE-02
1.540	−0.027	0.069	−0.067	2.451	5.80	−15.016	37.817	−31.167	9.261	1.42
1.541	−0.027	0.068	−0.066	2.450	5.58	−14.958	37.664	−31.033	9.223	1.44
1.542	−0.026	0.066	−0.065	2.449	5.39	−14.901	37.516	−30.902	9.186	1.45
1.543	−0.025	0.065	−0.064	2.447	5.22	−14.846	37.372	−30.776	9.150	1.46
1.544	−0.025	0.063	−0.063	2.446	5.08	−14.792	37.232	−30.654	9.116	1.47
1.545	−0.024	0.062	−0.062	2.444	4.97	−14.740	37.097	−30.535	9.083	1.48
1.546	−0.024	0.061	−0.061	2.443	4.88	−14.690	36.966	−30.421	9.051	1.49
1.547	−0.023	0.060	−0.060	2.441	4.80	−14.642	36.840	−30.310	9.020	1.50
1.548	−0.023	0.058	−0.059	2.440	4.73	−14.595	36.718	−30.203	8.990	1.51
1.549	−0.022	0.058	−0.058	2.439	4.64	−14.550	36.601	−30.100	8.961	1.52
1.550	−0.022	0.057	−0.058	2.437	4.50	−14.506	36.488	−30.001	8.933	1.53
1.551	−0.022	0.057	−0.058	2.436	4.26	−14.465	36.379	−29.906	8.907	1.54
1.552	−0.022	0.057	−0.058	2.435	3.88	−14.425	36.275	−29.814	8.881	1.55
1.553	−0.022	0.058	−0.058	2.434	3.39	−14.386	36.175	−29.726	8.856	1.56
1.554	−0.023	0.059	−0.059	2.433	2.95	−14.350	36.080	−29.642	8.833	1.56
1.555	−0.023	0.060	−0.061	2.432	2.78	−14.315	35.990	−29.562	8.810	1.57
1.556	−0.024	0.061	−0.061	2.431	2.85	−14.283	35.904	−29.485	8.789	1.58
1.557	−0.024	0.062	−0.062	2.430	2.97	−14.252	35.822	−29.413	8.769	1.58
1.558	−0.024	0.061	−0.062	2.429	3.03	−14.223	35.746	−29.344	8.749	1.59
1.559	−0.024	0.061	−0.061	2.428	3.01	−14.196	35.674	−29.279	8.731	1.60
1.560	−0.023	0.061	−0.061	2.427	2.96	−14.170	35.607	−29.219	8.714	1.60

5. Summary and Discussion

We have derived analytical approximations for the variation with the chemical potential of graphene of the effective indices and absorption coefficients of the fundamental TE and TM modes in three common types of silicon graphene waveguides. In all the cases a third-order polynomial provides an excellent degree of approximation ($<10^{-4}$) over the 1540–1560 nm wavelength band for the effective index. The approximation polynomials are useful in the process of device and subsystem design where one is interested in tuning their characteristics by applying suitable voltage control signals that, in turn, will change the chemical potential of the graphene layer(s) placed on top of the waveguide core. In this way, a given operation regime can be stated explicitly by a set of *N* required phase shift values:

$$\phi_i\left(\mu_{c,i}\right) = \frac{2\pi n_{eff,i}\left(\mu_{c,i}\right) L}{\lambda};\ i = 1, 2 \ldots N. \tag{8}$$

Starting from (8) and using (7) with the suitable coefficients for the operation wavelength and waveguide mode, one can obtain the required values of the chemical potentials. As we do not have access to experimental results, we can compare the results with those obtained in [12], which

TABLE V
Coefficients for the Fitting Polynomial [see (7)] for the TM Mode of Type-III Silicon Graphene Waveguide

	Effective Index (n_{eff})					Propagation Losses (dB/mm)				
λ (μm)	a	b	c	d	δE-05	a*	b*	c*	d*	δE-02
1.540	0.013	−0.021	−0.006	1.800	9.05	−40.951	105.25	−89.325	26.279	3.41
1.541	0.013	−0.022	−0.005	1.799	9.04	−40.048	103.01	−87.484	25.776	3.34
1.542	0.014	−0.022	−0.005	1.797	9.03	−39.177	100.85	−85.706	25.290	3.27
1.543	0.014	−0.023	−0.004	1.796	9.02	−38.336	98.763	−83.987	24.819	3.21
1.544	0.014	−0.024	−0.004	1.794	9.01	−37.524	96.743	−82.324	24.364	3.15
1.545	0.014	−0.024	−0.003	1.793	8.99	−36.738	94.788	−80.715	23.922	3.09
1.546	0.015	−0.025	−0.003	1.791	8.98	−35.978	92.895	−79.155	23.494	3.03
1.547	0.015	−0.025	—0.002	1.790	8.97	−35.241	91.062	−77.644	23.079	2.98
1.548	0.015	−0.026	−0.002	1.788	8.95	−34.528	89.284	−76.177	22.675	2.93
1.549	0.015	−0.026	−0.001	1.787	8.94	−33.836	87.559	−74.754	22.283	2.88
1.550	0.015	−0.027	−0.001	1.785	8.93	−33.165	85.885	−73.372	21.902	2.83
1.551	0.016	−0.027	0.000	1.784	8.91	−32.514	84.260	−72.029	21.532	2.78
1.552	0.016	−0.028	0.000	1.783	8.90	−31.881	82.681	−70.723	21.171	2.74
1.553	0.016	−0.028	0.001	1.781	8.88	−31.267	81.145	−69.454	20.820	2.69
1.554	0.016	−0.029	0.001	1.780	8.87	−30.670	79.653	−68.218	20.478	2.65
1.555	0.016	−0.029	0.002	1.778	8.85	−30.089	78.200	−67.016	20.145	2.61
1.556	0.017	−0.030	0.002	1.777	8.84	−29.524	76.787	−65.845	19.820	2.57
1.557	0.017	−0.030	0.002	1.776	8.82	−28.974	75.411	−64.704	19.504	2.53
1.558	0.017	−0.031	0.003	1.774	8.81	−28.439	74.070	−63.593	19.195	2.49
1.559	0.017	−0.031	0.003	1.773	8.79	−27.918	72.764	−62.509	18.893	2.46
1.560	0.017	−0.032	0.004	1.771	8.77	−27.410	71.492	−61.453	18.599	2.42

is the most complete work reported so far for electro-refractive modulation using graphene. In this sense, for type-II waveguides the refractive index variation is in the 10^{-4} orders of magnitude while for the type III is in the 10^{-3} orders of magnitude. In both cases these orders are within the same range as those reported in the paper. The approximation derived in the paper can therefore be applied for the design of a wide range of silicon graphene integrated devices ranging from simple configurations such as tunable polarization filters and dividers to complex electro-refractive modulators and finite/infinite impulse response tunable filters.

As mentioned before, the polynomial approximation is linked to specific waveguide designs. In this respect, we wish to point out that we have focused on three particular designed that have been proposed in the literature of which, type-III is the most efficient in terms of refractive index modulation. The method outlined here can, however, be expanded following the guidelines described in Section IV.1 and Fig. 3 to investigate other waveguide designs and obtain suitable polynomial approximations.

References

[1] A. K. Geim and K. S. Novoselov, "The rise of graphene," *Nature Mater.*, vol. 6, pp. 183–191, 2007.
[2] A. Vakil and N. Engheta, "Transformation optics using graphene," *Science*, vol. 332, pp. 1291–1294, 2008.
[3] B. Sensale-Rodriguez, R. Yan, L. Liu, D. Jena, and H. G. Xing, "Graphene for reconfigurable THz optoelectronics," *Proc. IEEE*, vol. 107, no. 7, pp. 1705–1716, Jul. 2013.
[4] F. Bonnacorso, Z. Sun, T. Hasan, and A. C. Ferrari, "Graphene photonics and optoelectronics," *Nature Photon.*, vol. 4, pp. 611–622, 2010.
[5] B. Sensale-Rodriguez, "Graphene based optoelectronics," *IEEE J. Lightw. Technol.*, vol. 32, pp. 1100–1108, 2015.
[6] M. Liu *et al.*, "A graphene-based broadband optical modulator," *Nature*, vol. 474, pp. 64–67, 2011.
[7] M. Liu, X. Yin, and X. Zhang, "Double-layer graphene optical modulator," *Nano Lett.*, vol. 12, pp. 1482–1485, 2012.
[8] Z. Lu and L. Zhao, "Nanoscale electro-optic modulators based on graphene-slot waveguides," *J. Opt. Soc. Amer. B*, vol. 6, pp. 1490–1496, 2012.
[9] M. Midrio *et al.*, "Graphene-assisted critically-coupled optical ring modulator," *Opt. Exp.*, vol. 20, pp. 23144–23155, 2012.
[10] L. Yang *et al.*, "Proposal for a 2×2 optical switch based on graphene-silicon-waveguide microring," *IEEE Photon. Tech. Lett.*, vol. 26, no. 3, pp. 235–238, Feb. 2014.
[11] C. Xu, Y. Jin, L. Yang, J. Yang, and X. Jiang, "Characteristics of electro-refractive modulating based on graphene-oxide-silicon waveguide," *Opt. Exp.*, vol. 20, pp. 22398–22405, 2012.
[12] V. Sorieanello, M. Midrio, and M. Romagnoli, "Design of single and double layer graphene phase modulators in SOI," *Opt. Express*, vol. 23, pp. 6478–6490, 2015.
[13] M. Midrio, P. Galli, M. Romagnoli, L. C. Limerling, and J. Michel, "Graphene-based optical phase modulation of waveguide transverse electric modes," *Photon. Res.*, vol. 2, no. 3, pp. A34–A40, 2014.
[14] M. Moshin *et al.*, "Experimental verification of electro-refractive phase modulation in graphene," *Sci. Rep.*, vol. 5, 2015, Art. no. 10967.
[15] J. Capmany, D. Domenech, and P. Muñoz, "Silicon graphene waveguide tunable broadband microwave photonics phase shifter," *Opt. Exp.*, vol. 22, pp. 8094–8100, 2014.
[16] J. Capmany, D. Domenech, and P. Muñoz, "Silicon graphene reconfigurable CROWS and SCISSORS," *IEEE Photon. J.*, vol. 7, no. 2, pp. 1–9, Apr. 2015.
[17] J. Capmany, D. Doménech, and P. Muñoz, "Graphene integrated microwave photonics," *J. Lightw. Technol.*, vol. 32, no. 20, pp. 3785–3796, Oct. 2014.
[18] M. Ndeljkovic, R. Soref, and G. Z. Mashanovich, "Free-carrier electrorefraction and electroabsorption modulation predictions for silicon over the 1-14 mm infrared wavelength range," *IEEE Photon. J.*, vol. 3, no. 6, pp. 1171–1180, Dec. 2011.
[19] G. W. Hanson, "Dyadic Green's function and guided surface waves for a surface conductivity model of graphene, " *J. Appl. Phys*, vol. 103, 2008, Art. no. 064302.